

Si *K*-edge XANES study of $\text{SiO}_x\text{C}_y\text{H}_z$ amorphous polymeric materials

J. Chaboy

Instituto de Ciencia de Materiales de Aragón, CSIC-Universidad de Zaragoza, 50009 Zaragoza, Spain

A. Barranco, A. Yanguas-Gil, F. Yubero, and A. R. González-Elipe

*Instituto de Ciencia de Materiales de Sevilla, CSIC-Universidad Sevilla,**and Departamento de Química Inorgánica, Avenida Américo Vespucio s/n, E-41092 Sevilla, Spain*

(Received 22 June 2006; revised manuscript received 31 October 2006; published 22 February 2007)

This work reports on x-ray absorption spectroscopy study at the Si *K* edge of several amorphous $\text{SiO}_x\text{C}_y\text{H}_z$ polymers prepared by plasma-enhanced chemical-vapor deposition with different C/O ratios. SiO_2 and SiC have been used as reference materials. The comparison of the experimental Si *K*-edge x-ray absorption near-edge structure spectra with theoretical computations based on multiple scattering theory has allowed us to monitor the modification of the local coordination around Si as a function of the overall C/O ratio in this kind of materials.

DOI: 10.1103/PhysRevB.75.075205

PACS number(s): 61.10.Ht, 81.05.-t, 81.15.Gh, 81.07.Pr

I. INTRODUCTION

Silicone-like amorphous materials with $\text{SiO}_x\text{C}_y\text{H}_z$ compositions prepared by either chemical methods¹ or plasma processes² have found many applications in a large variety of fields.^{3–5} Modulation of the properties of these types of materials is possible by changing the composition (i.e., Si:O:C:H ratio) or the atom distribution within their polymer structure.⁶ Thus, for example, their optical and dielectric properties, their barrier diffusion behavior, or their wetting properties can be tailored by modifying their structure and/or the type of functional groups at the surface. Generally, the structure of these polymers is characterized by means of infrared spectroscopy⁷ and x-ray photoemission spectroscopy.⁸ More recently, the use of synchrotron radiation has been incorporated to the methods currently available to structurally characterize $\text{SiO}_x\text{C}_y\text{H}_z$ and other silicon containing compounds.^{9–11} A key issue of this structural characterization is the determination of the local coordination arrangement around the Si, as this local structure is critical for the determination of the dielectric and optical properties of this type of materials.¹²

In the present work, we face the structural determination of the local environment around Si in a series of amorphous $\text{SiO}_x\text{C}_y\text{H}_z$ thin films prepared by plasma-enhanced chemical-vapor deposition (PECVD), where the C/O ratio in the films has been controlled by conveniently adjusting the deposition conditions. We have studied the x-ray absorption near-edge spectroscopy (XANES) at the Si *K* edge in order to monitor possible modifications of the Si neighborhood as a function of the different C/O ratios. In this way, we have performed a careful theoretical analysis of the Si *K*-edge XANES spectra by assuming distorted SiO(C) coordinations with a total number of four oxygen and carbon atoms around the silicon (i.e., tetrahedral coordination). The analysis has permitted us to establish a clear correlation between the different spectral features and the local structure around Si in this kind of $\text{SiO}_x\text{C}_y\text{H}_z$ amorphous materials.

II. EXPERIMENT AND METHODS

The $\text{SiO}_x\text{C}_y\text{H}_z$ thin films studied here have been prepared by PECVD. Details about the preparation protocol can be

found in Refs. 13 and 14. A single crystal of SiC and a SiO_2 thin film grown by PECVD¹³ have been used as reference samples. The composition of the silicone-like films has been determined by Rutherford backscattering spectroscopy (RBS) and elastic recoil dispersion analysis (ERDA) at the ion accelerator of ARAMIS (Orsay, France).

For the present study, we have selected five samples whose compositions and C/O atomic ratios are summarized in Table I. It is worth noting that the reported compositions correspond to the overall atomic content in the films, but this does not imply that the number of Si–C and Si–O bonds should reflect the reported values. XANES spectra were recorded at the Si *K* absorption edge at the SA32 beamline in the SuperACO synchrotron (LURE, Orsay, France). A InSb(111) double crystal monochromator was used for the selection of photon energies (resolution of 0.75 at 2000 eV). The spectra were recorded by measuring the drain current through the samples (i.e., total electron yield detection).

The absorption spectra were analyzed according to standard procedures. Extended x-ray-absorption fine structure (EXAFS) oscillations were obtained from the x-ray-absorption spectra by subtracting a Victoreen curve followed by a cubic spline background removal using the program AUTOBK.¹⁵ The obtained signal, $\chi(k)$, was normalized to the edge jump. In all cases, Fourier transform has been performed by weighting the EXAFS signals by the wave number in the *k* range $2 \leq k \leq 11.8$, multiplying $\chi(k) \cdot k$ by a Kaiser-Bessel window and without phase correction.

TABLE I. Composition and C/O atomic ratio of polymeric thin films as determined by RBS/ERDA.

Sample	Composition	C/O atomic ratio
C	$\text{SiO}_{0.7}\text{C}_4\text{H}_9$	5.7
C'	$\text{SiO}_{1.2}\text{C}_{1.5}\text{H}_3$	4.1
B	$\text{SiO}_2\text{C}_{4.7}\text{H}_7$	2.3
A	$\text{SiO}_{1.5}\text{C}_{1.5}\text{H}_{1.8}$	1
A'	$\text{SiO}_{1.5}\text{C}_{1.5}\text{H}_3$	1

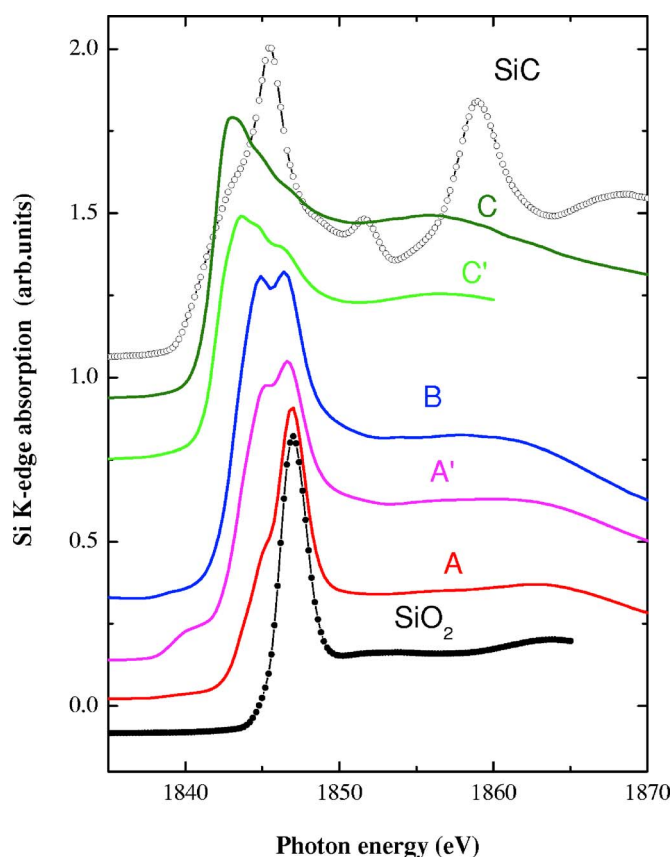


FIG. 1. (Color online) Comparison of the Si K -edge XANES spectra of cubic 3C-SiC (black, \circ), SiO₂ (black, \bullet) and the SiO_{*x*}C_{*y*}H_{*z*} compounds. The spectra have been vertically shifted for the sake of clarity.

The computation of the Si K -edge XANES spectra was carried out by using the multiple-scattering code CONTINUUM based on the one-electron full-multiple-scattering theory.¹⁶ A complete discussion of the procedure can be found in Ref. 17. Regarding the specific details of the computations, we have taken advantage of the previous work performed in α quartz and α -SiO₂,¹⁸ where an extensive discussion of the computational methods of the Si K -edge spectra can be found. Accordingly, (i) the muffin-tin radii were chosen following Norman's criterion with a 10% overlapping factor and (ii) the final state potential was built up following the screened and relaxed $Z+1$ approximation, with its exchange and correlation parts (ECP) computed by using the real part of the Hedin-Lundqvist (HL) potential. The calculated theoretical spectra have been further convoluted with a Lorentzian shape function to account for the core-hole lifetime and the experimental resolution.

III. RESULTS AND DISCUSSION

A. Si K -edge XANES and EXAFS spectra

The Si K -edge XANES spectra of the SiO_{*x*}C_{*y*}H_{*z*} compounds are shown in Fig. 1. They are compared with those of the SiO₂ and SiC reference compounds. The Si K edge in the SiO₂ thin film shows a strong and narrow white line and a

broad structure at ~ 20 eV above the white line. By contrast, the Si K -edge spectrum of SiC exhibits several absorption features. In particular, its ~ 10 eV wide main absorption line shows a shoulderlike contribution at the low-energy side. In addition, there are both a weak feature and a huge resonance at ~ 6 and ~ 14 eV above the main peak, respectively. Hence, despite the fact that similar to the SiO₂ case, the first neighboring arrangement around Si in SiC is also tetrahedral, it seems that in this compound the contribution from further shells to the XANES spectrum is rather significant.

The SiO_{*x*}C_{*y*}H_{*z*} compounds exhibit a XANES spectrum whose shape is quite different from either that of SiC or that of SiO₂. Similar to the amorphous SiO₂, all the spectra are characterized by a main absorption line without any additional spectral feature for energies above the edge. In a first approach, this result confirms the expected short-range order for the coordination of Si in the SiO_{*x*}C_{*y*}H_{*z*} compounds. However, the shape of the main line is markedly different for all the studied samples. Surprisingly, the spectral shape is very different for A and A' samples despite the fact that both contain the same C/O ratio. Indeed, the spectral profile of sample A' is more similar to that of sample B that is characterized by an intermediate value of the C/O ratio and that exhibits a split main absorption line. In this regard, it should be noted that the similar C/O ratio depicted by samples A and A' does not necessarily imply that they present the same type of local coordination around silicon. XANES spectra of samples C and C', showing the highest C/O ratio, resemble that of an amorphous Si_{1-*x*}C_{*x*}:H alloy.¹⁹ It is interesting to note that by annealing at high temperatures of this alloy compound, it releases hydrogen and renders crystalline SiC with a XANES spectrum similar to that of the C' compound in Fig. 1. Based on these results, it is likely that in polymers C and C' the first coordination sphere around silicon mainly consists of C atoms.

Trying to get a deeper insight into the modifications of the local environments in the SiO_{*x*}C_{*y*}H_{*z*} films of Si with different C/O ratios we have studied the Si K -edge EXAFS signals. Figure 2 shows a comparison of the EXAFS spectra for samples A–C and that of the reference SiO₂ compound. Sample A belongs to the group of polymers showing the smallest C/O ratio; in sample B, the C/O ratio is intermediate, while the highest ratio is found in sample C. As shown in Fig. 2, the $\chi(k) \cdot k$ signals of samples with intermediate (Sample B) and low (Sample A) ratios resemble that of SiO₂. This is evidenced by the similar frequency of the EXAFS oscillation in all the cases. Differences are found in the amplitude of the signal, which is reduced for the polymers, and in the shape of the feature centered at $\sim 4.5 \text{ \AA}^{-1}$. By contrast, sample C shows modified amplitudes and frequencies along the whole EXAFS spectral region. These results suggest that the local environment of Si in samples A and B is similar to that of SiO₂, being modified for higher C/O ratios.

To clearly show the differences and similarities among our samples and the SiO₂, it is instructive to compare the Fourier transform of the EXAFS spectra. This is shown in Fig. 1 for samples A–C, as well as for the reference SiO₂. The Fourier transform (FT) signals of both samples A and B are characterized by a main peak at the position of the first coordination shell. These curves resemble the FT spectrum

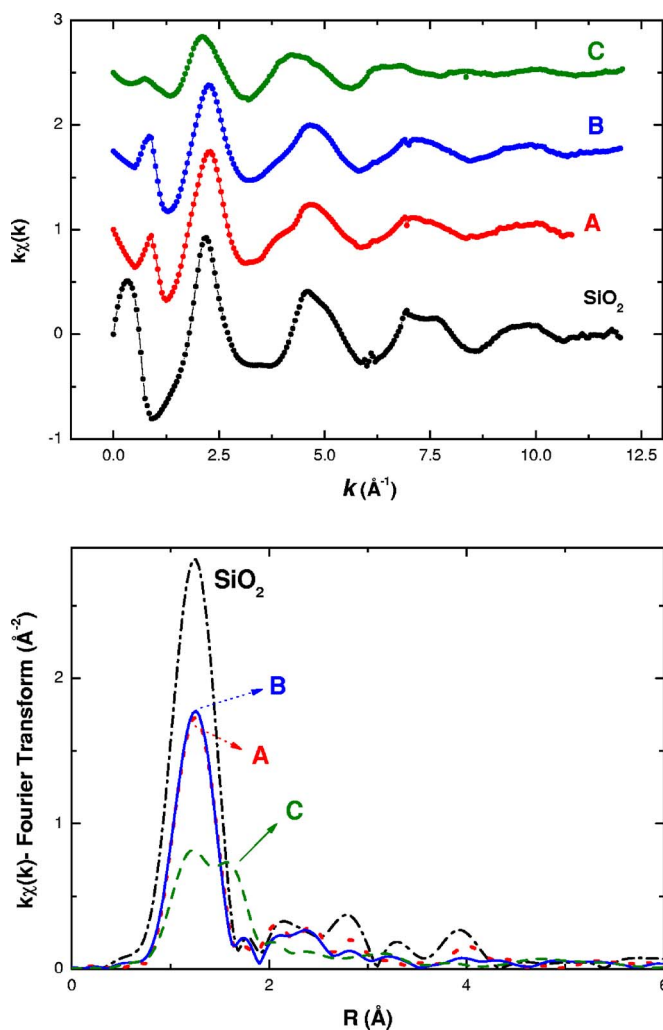


FIG. 2. (Color online) (Top panel) Experimental k -weighted EXAFS signals of SiO_2 (black) and different $\text{SiO}_x\text{C}_y\text{H}_z$ samples: A (red), B (blue), and C (green). The spectra are displayed by using the same scale and they have been vertically shifted for the sake of clarity. (Bottom panel) Comparison of the modulus of the Fourier transform of the experimental Si K -edge k -EXAFS spectra of SiO_2 (black, dash-dotted) and $\text{SiO}_x\text{C}_y\text{H}_z$ samples: A (red, dots), B (blue, solid line), and C (green, dash).

of SiO_2 except for the slightly smaller intensity of the first coordination peak that would indicate a less ordered arrangement of the first coordination atoms around Si. By contrast, sample C is characterized by a radial distribution where two well-differentiated peaks can be distinguished in the first coordination feature. This seems to indicate that the atom arrangement around Si is very distorted with O and C atoms at different bond distances towards Si. While this latter conclusion is in agreement with a fingerprint assignment of the XANES spectra, a similar evidence is not found for the low and intermediate C/O ratio samples (see Fig. 1). Indeed, while EXAFS of samples A and B points out the existence of a single coordination shell around Si, XANES indicates that in these samples the Si environment is significantly modified with respect to that of SiO_2 . One possibility to account for such an apparent contradiction is that as the C/O increases some C atoms bond directly to Si substituting oxygen from

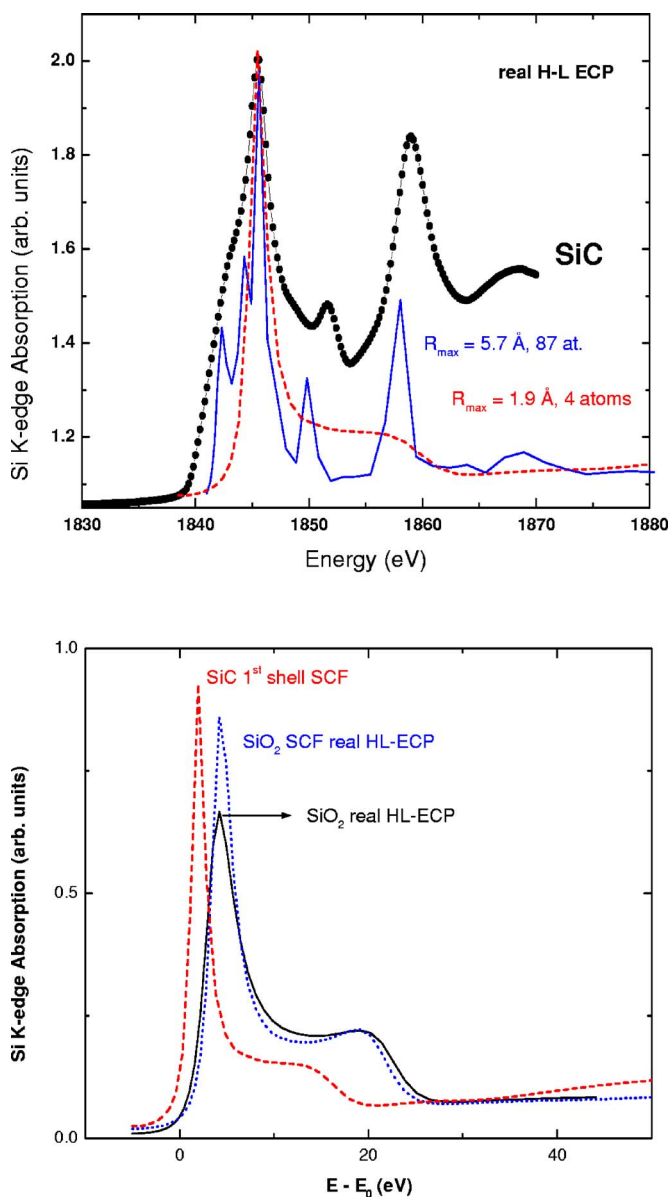


FIG. 3. (Color online) (Top) Comparison of the experimental Si K -edge XANES of cubic 3C-SiC (black, \bullet) and the theoretical spectra computed by using a real Hedin-Lundqvist ECP for a cluster containing 87 atoms (blue, solid line). The calculated spectrum for the first neighboring shell is also shown (red, dotted line). (Bottom) Comparison of the theoretical Si K -edge XANES spectra computed for the first coordination shell in both amorphous a - SiO_2 (black, solid line) and 3C-SiC (red, dashed). In the case of a - SiO_2 , the same computation performed by using a self-consistent-field real Hedin-Lundqvist potential is shown (blue, dotted line).

the first coordination sphere. In this way, two different Si-C and Si-O contributions would be observed in the XANES spectra although the difference in the interatomic distances would not be large enough to yield a splitted peak in the first peak of Fourier transform of the EXAFS signals.

B. Theoretical computation of the Si K -edge XANES spectra

To account for the origin of such a peculiar behavior, we have performed *ab initio* calculations of the Si K -edge

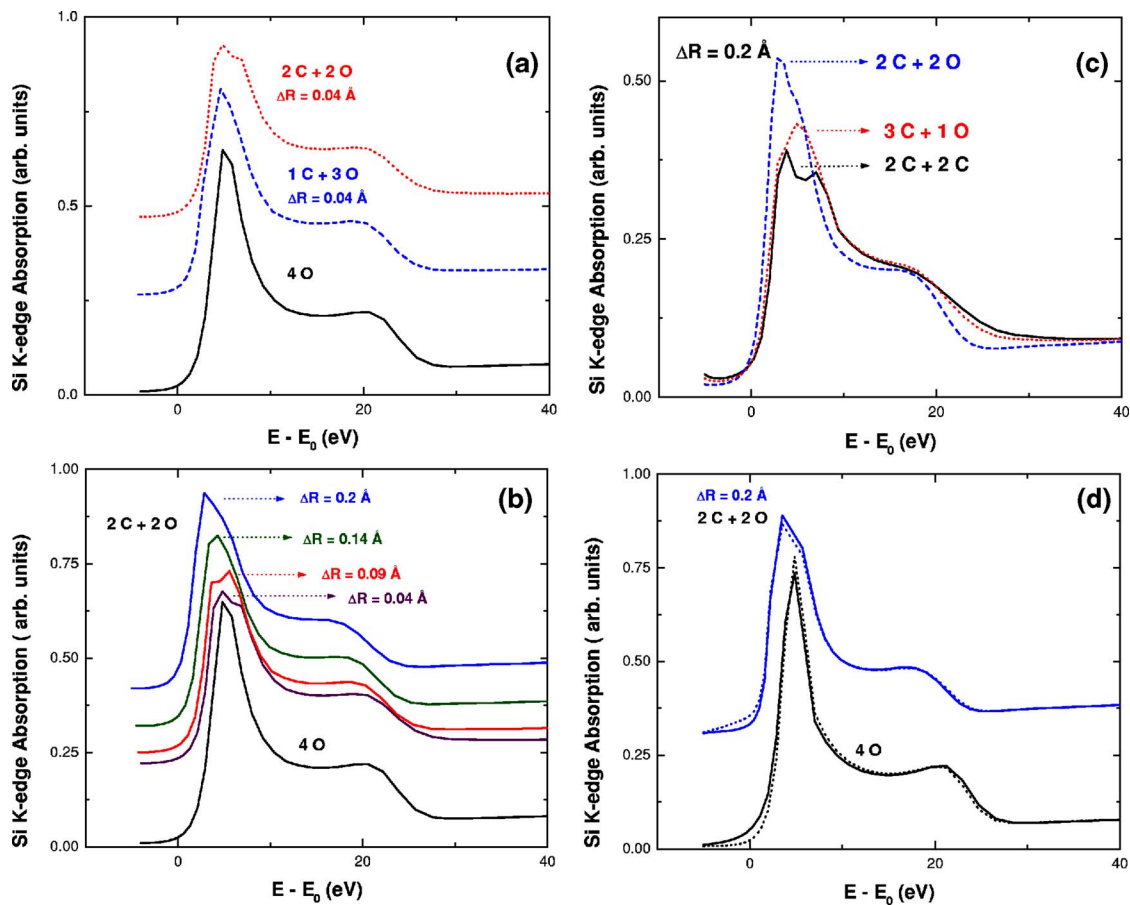


FIG. 4. (Color online) (a) Comparison of the theoretical Si *K*-edge XANES spectra computed for regular *a*-SiO₂ (black, solid line) and the distorted structures ($\Delta R=0.04 \text{ \AA}$) in which C substitutes O atoms: 2O+2C (red, dots) and 3O+1C (blue, dashed). (b) Comparison of the theoretical Si *K*-edge XANES spectra computed for regular *a*-SiO₂ (black, solid line) and the distorted 2O+2C structures with $\Delta R=0.04 \text{ \AA}$ (purple), 0.09 \AA (red), 0.14 \AA (green), and 0.2 \AA (blue). (c) Comparison of the theoretical Si *K*-edge XANES spectra computed for the distorted structures ($\Delta R=0.2 \text{ \AA}$) with different C-O substitutions: 2O+2C (blue), 3O+1C (red), and 2C+2C (black). (d) Comparison of the theoretical Si *K*-edge XANES spectra computed for regular *a*-SiO₂ (black, solid line) and the distorted 2O+2C structure with $\Delta R=0.2 \text{ \AA}$ (blue, solid line) and for the same clusters adding 4H atoms in collinear Si-O-H and Si-C-H arrangements (dotted lines). For the sake of clarity, no broadening has been applied to the computed signals.

XANES. Firstly, calculations have been performed for the reference compounds SiC and amorphous SiO₂. Figure 3 reports the comparison of the experimental Si *K*-edge XANES spectrum of SiC and that computed for a cluster including atoms (87) located within a maximum interatomic distance of 5.7 \AA around silicon. In the same figure, we show the simulation performed for a small cluster that includes only the first (4C) coordination shell around Si. This comparison illustrates the long-range origin of the experimental spectral features appearing beyond the main absorption line. Indeed, as shown in Fig. 3, the contribution of the first coordination shell in both SiC and *a*-SiO₂ is similar. In both cases, the first nearest neighbors around the absorbing Si atom are arranged forming a tetrahedron. Therefore, the only difference in these clusters is, in addition to the interatomic distance, the nature of the neighbor atom (C vs O). It is also interesting to note that the spectral profile is mainly governed by the tetrahedral geometry, so that if one tries to improve the computations by using self-consistent-field (SCF) final-state potentials, only the height and not the shape of the white line is affected.

The results of these calculations suggest that the behavior of the Si *K*-edge absorption in the SiO_xC_yH_z polymeric materials is not exclusively linked to a simple substitution of O by C atoms as the C/O ratio increases. In addition, the observed departure from the spectral shape of *a*-SiO₂ also results from a modification of the interatomic distances in a tetrahedral arrangement. Therefore, we have considered both the distortion of the tetrahedron and the substitution of O by C atoms. In this way, Fig. 4(a) shows the comparison of the computed XANES for the undistorted Si-4O cluster, and the spectra calculated for clusters with a slight distortion ($\Delta R=0.04 \text{ \AA}$) and different C-O substitutions. For such a distortion, as shown in the figure, when one C atoms enters in the neighborhood of Si, the width of the main absorption line increases. Moreover, the effect of two C atoms placed at the largest ($\Delta R=0.04 \text{ \AA}$) distance yields a splitting of the white line. It should be noted that both the slight distortion and the C-O substitution only modify the main absorption line without affecting the high-energy region. This result is in agreement with the unvarying line shape observed for the

EXAFS spectra of the $\text{SiO}_x\text{C}_y\text{H}_z$ compounds with low (A and A') and intermediate (B) C/O ratios.

Then, we proceeded to increase the distortion of the tetrahedron for a fixed C-O substitution. The results are shown in Fig. 4(b) for a 2O+2C arrangement and a maximum distortion of 0.2 Å. The modification of the Si K-edge absorption profile strongly resembles the experimental trend reported in Fig. 1. This result points out that, in all the cases, the effect of the C-O substitution induces a distortion in the first neighboring tetrahedron around Si although the smallest distortions are below the sensitivity of the EXAFS technique to detect two different contributions in the first coordination sphere. Finally, we tested the effect of the different C-O substitutions on the maximum allowed distortion of the tetrahedron. As shown in Fig. 4(c), the height of the main absorption line decreases as the C content increases. For the complete substitution of O by C, i.e., a 4C atoms environment with two different distances, a second peak appears at the high-energy side of the white line. This profile reproduces the experimental XANES observed for both C and C' compounds. For the sake of completeness, we have performed the calculations on the same clusters but adding hydrogen atoms bonded ($d \sim 1.1$ Å) to both O and C ones in collinear Si-O-H and Si-C-H arrangements. For such an arrangement, one expects the maximum contribution of H atoms to the XANES spectra. However, as shown in panel d of Fig. 4, the addition of hydrogen atoms does not account for the observed experimental trend.

The scenario emerging from this XANES analysis is that the tetrahedron coordinating Si in compounds C and C' is the carbon richest ($\sim 4\text{C}$ atoms) and the most distorted, $0.1 \leq \Delta R \leq 0.2$ Å, within the series. For compounds B and A', the comparison of the computed and experimental spectra suggests the occurrence of a distorted tetrahedron $\Delta R \leq 0.1$ Å in which the long distance corresponds to two carbon atoms. This effect seems less intense for compound A. In this case, the number of oxygen atoms around silicon must be higher than two, thus defining a local coordination approaching that of SiO_2 . This picture suggests that the dis-

ortion increases with C content, in agreement with the fact that the interatomic Si-C distance in SiC is greater than the Si-O one in $a\text{-SiO}_2$.

IV. SUMMARY AND CONCLUSIONS

In this work, we have presented a study based on the x-ray absorption spectra at the Si K edge of $\text{SiO}_x\text{C}_y\text{H}_z$ polymers with variable C/O ratios. The presence of carbon atoms directly bonded to Si modifies the local environment around this atom. For low C/O ratios in the compounds, no unambiguous conclusions can be obtained regarding the Si-C and Si-O arrangements based only on the EXAFS information. Information on this point can be obtained by detailed *ab initio* multiple-scattering calculations of the Si K-edge XANES of these systems. The comparison between the experimental XANES spectra and the results of the computations has shown that the peculiar behavior of the Si K-edge XANES spectra of these materials can be accounted for by considering both the substitution of oxygen by carbon atoms in the SiO_4 tetrahedron existing in $a\text{-SiO}_2$ and its concomitant structural distortion. Thus, the intensity ratio of the first and second peaks sometimes appearing in the Si K absorption edge can be considered as a fingerprint for a semiquantitative evaluation of the number of Si-C and Si-O bonds present in the samples. This information is interesting since many technological properties of this type of material strongly depend on this local coordination rather than on the actual composition of the films.

ACKNOWLEDGMENTS

This work was partially supported by the Spanish CICYT (Grants MAT2005-06806-C04-04 and MAT2004-01558). The x-ray absorption spectra have been measured in LURE (Paris) under the EU large facility program. We thank C. Clerc and R. J. Prado for their assistance in the RBS/ERDA and XANES measurements, respectively.

¹S. Meth and C. N. Sukenik, *Thin Solid Films* **425**, 49 (2003).

²A. M. Wróbel and M. R. Werthamer, in *Plasma Deposition, Treatment and Etching of Polymers*, edited by R. d'Agostino (Academic Press, Boston, 1990), Chap. 3.

³C. A. Vienna, N. I. Morino, and O. Bunnaud, *Microelectron. Reliab.* **40**, 613 (2000).

⁴F. Benítez, E. E. Martínez, and J. Esteve, *Thin Solid Films* **377&378**, 109 (2000).

⁵K. Li and J. Meichsner, *Surf. Coat. Technol.* **116–119**, 841 (1999).

⁶Q. Wu and K. K. Gleason, *J. Vac. Sci. Technol. A* **21**, 388 (2003).

⁷M. F. A. M. van Hest, A. Klaver, D. C. Schram, and M. C. M. van de Sandan, *Thin Solid Films* **449**, 10 (2004).

⁸Y. Wu, M. Bekke, Y. Inoue, H. Sugimura, H. Kitaguchi, C. Liu, and O. Takai, *Thin Solid Films* **457**, 122 (2004).

⁹A. Barranco, J. Cotrino, F. Yubero, T. Girardeau, S. Camelio, and

A. R. González-Elipse, *Surf. Coat. Technol.* **180&181**, 244 (2004).

¹⁰S. Bender, R. Franke, E. Hertmann, V. Lansmann, M. Jansen, and J. Hornes, *J. Non-Cryst. Solids* **298**, 99 (2002).

¹¹R. Franke, C. Girgenrath, S. Kohn, M. Jansen, and J. Fresenius, *Anal. Chem.* **361**, 587 (1998).

¹²K. Maex, M. R. Baklanov, D. Shamiryan, F. Iacopi, S. H. Brongersma, and Z. S. Yanovitskaya, *J. Appl. Phys.* **93**, 8793 (2003).

¹³A. Walkiewicz-Pietrzykowska, J. Cotrino, and A. R. González-Elipse, *Chem. Vap. Deposition* **11**, 317 (2005).

¹⁴A. Barranco, J. Cotrino, F. Yubero, J. P. Espinós, J. Benítez, C. Clerc, and A. R. González-Elipse, *Thin Solid Films* **401**, 150 (2001).

¹⁵M. Newville, P. Livins, Y. Yacoby, J. J. Rehr, and E. A. Stern, *Phys. Rev. B* **47**, 14126 (1993).

¹⁶C. R. Natoli and M. Benfatto (unpublished); M. Benfatto, C. R.

- Natoli, A. Bianconi, J. García, A. Marcelli, M. Fanfoni, and I. Davoli, *Phys. Rev. B* **34**, 5774 (1986).
- ¹⁷C. Natoli, M. Benfatto, S. D. Longa, and K. Hatada, *J. Synchrotron Radiat.* **10**, 26 (2003).
- ¹⁸J. Chaboy, M. Benfatto, and I. Davoli, *Phys. Rev. B* **52**, 10014 (1995).
- ¹⁹R. J. Prado, T. F. D'addio, M. C. A. Fantini, I. Pereyra, and A. M. Flank, *J. Non-Cryst. Solids* **330**, 196 (2003).